frontiers | Frontiers in Marine Science

TYPE Original Research
PUBLISHED 10 October 2023
DOI 10.3389/fmars.2023.1124763

OPEN ACCESS

EDITED BY
Riccardo Briganti,
University of Nottingham, United Kingdom

REVIEWED BY
Giovanni Besio,
University of Genoa, Italy
Gioele Ruffini,
Sapienza University of Rome, Italy

*CORRESPONDENCE
Joan Pau Sierra
joan.pau.sierra@upc.edu

RECEIVED 20 February 2023
ACCEPTED 25 September 2023
PUBLISHED 10 October 2023

CITATION
Sierra JP, Sánchez-Arcilla A, Gironella X, Gracia V, Altomare C, Mösso C, González-Marco D, Gómez J, Barceló M and Barahona C (2023) Impact of climate change on berthing areas in ports of the Balearic Islands: adaptation measures. *Front. Mar. Sci.* 10:1124763. doi: 10.3389/fmars.2023.1124763

Impact of climate change on berthing areas in ports of the Balearic Islands: adaptation measures

Joan Pau Sierra[1,2]*, Agustín Sánchez-Arcilla[1,2], Xavier Gironella[1,2], Vicente Gracia[1,2], Corrado Altomare[1,2], César Mösso[1,2], Daniel González-Marco[1,2], Jesús Gómez[1,2], Mateo Barceló[3] and Cristina Barahona[3]

[1]Laboratori d'Enginyeria Marítima, Universitat Politècnica de Catalunya BarcelonaTech, Barcelona, Catalonia, Spain, [2]Centre Internacional d'Investigació dels Recursos Costaners (CIIRC), Barcelona, Catalonia, Spain, [3]Servei d'Explotació, Projectes i Obres, Ports de les Illes Balears, Palma, Balearic Islands, Spain

Climate change generates impacts on coastal areas due to sea-level rise and potential modifications in wave and storm surge patterns. Since harbours are located in littoral areas, they will experience different impacts associated to such processes. In this paper, the effects of climate change on port berthing areas in terms of operability are quantified. The study is focused on the ports of the Balearic Islands (Western Mediterranean Sea) and analyses the loss of operability due to the reduction of freeboard in berthing structures and the potential variation in agitation within these harbours during the 21st century, considering two different climate scenarios (RCP4.5 and RCP8.5) and two-time horizons (2045 and 2100). In addition, adaptation measures to address such impacts are proposed and their cost estimated. The results indicate that climate change will not generate significant changes in wave agitation due to negligible variations in wave patterns under future scenarios. On the contrary, sea-level rise will cause huge increases of inoperability for berthing structures due to insufficient freeboard: 10.5% under RCP4.5 or 20.5% under RCP8.5 in 2045, increasing to 57.1% (RCP4.5) and even 83.2% (RCP8.5) in 2100.

KEYWORDS

climate change, sea-level rise, port agitation, port operability, adaptation measures, Balearic Islands

1 Introduction

Climate change triggers a number of potential hazards and impacts on coastal areas (Sierra and Casas-Prat, 2014) which are climate-sensitive systems with a high vulnerability (Nicholls et al., 2011; Sánchez-Arcilla et al., 2011; Vitousek et al., 2017; Grases et al., 2020; Vousdoukas et al., 2020). One of the most evident consequences of the global warming

induced by climate change is sea level rise (SLR), mainly due to thermal volume expansion and land ice melting (e.g. Pritchard and Vaughan, 2007; Gregory et al., 2013; Dangendorf et al., 2017; Vousdoukas et al., 2018). According to projections, SLR will differ substantially among different coastal areas due to the spatial variation of the mechanisms contributing to it (Scarascia and Lionello, 2013; Slangen et al., 2014; Durand et al., 2022). In spite of the great uncertainty associated to future SLR projections, numerous authors have estimated its impacts on coastal areas (e.g. Nicholls and Cazenave, 2010; Revell et al., 2011; Vousdoukas et al., 2012; Brown et al., 2013; Brown and Nicholls, 2015; Hinkel et al., 2015; Ranasinghe, 2016; Enríquez et al., 2017; Enríquez et al., 2019; Bon de Sousa et al., 2018; Sayol and Marcos, 2018; Orejarena-Rondón et al., 2019; Grases et al., 2020; Agulles et al., 2021; Luque et al., 2021), because it generates geomorphological changes such as flooding and erosion that threaten infrastructures and other assets located in the coastal fringe.

Although vulnerability of coastal areas is normally assessed focusing on SLR, other non-climatic drivers as socioeconomic change are often ignored, despite being fundamental for coastal management associated to climatic impacts (Nicholls et al., 2008). Moreover, there are other physical processes that can also generate impacts on these coastal areas. The greenhouse effect, in addition to SLR, may generate changes in wind and atmospheric pressure patterns, which, in turn, can modify storm surge (Conte and Lionello, 2013; Rahmstorf, 2017; Bevacqua et al., 2019; Li et al., 2020; Hsiao et al., 2021; Cousineau and Murphy, 2022; Leal et al., 2022) and sea wave patterns (Hemer et al., 2013a; Hemer et al., 2013b; Hemer and Trenham, 2016; Casas-Prat et al., 2018; Bonaldo et al., 2020; Meucci et al., 2020; Lobeto et al., 2021a; Morim et al., 2021; Goharnejad et al., 2022). Thus, for example, Casas-Prat et al. (2018) results project lower waves in the North Atlantic and an increase of wave heights in the Southern Hemisphere. These higher waves are accompanied with increased peak wave period and a significant counterclockwise rotation in the mean wave direction in the Southern Oceans. Meucci et al. (2020) also found that the magnitude of the extreme wave heights would increase over the Southern Ocean by the end of the 21st century and in the North Atlantic would decrease at low to mid latitudes and would increase at high latitudes. In the same way, Lobeto et al. (2021a) and Morim et al. (2021) obtained similar results.

In the specific case of harbors, since they are located in coastal areas, climate change will result in a range of different impacts (Sánchez-Arcilla et al., 2016; Izaguirre et al., 2021). Considering that ports play an essential role in the global economy as transportation hubs and their contribution to economic activities is very significant, in particular in the coastal fringe and their hinterland, the impacts of climate change on ports are one of the main climatic risks in littoral zones (Becker et al., 2012; Izaguirre et al., 2021).

Since wave storms strongly hinder port activities (de Alfonso et al., 2021) and some authors project a greater frequency of extreme events (Mitchell et al., 2006; Stott, 2016), the consequences for harbor operations may be adverse. Changes in wave storm patterns may affect port agitation (Casas-Prat and Sierra, 2012; Sierra et al., 2015; Sierra et al., 2017; Campos et al., 2019; Camus et al., 2019; Lesani and Niksokhan, 2019), port breakwater stability (Takagi et al., 2011; Mase et al., 2013; Suh et al., 2013) or port siltation (Sierra and Casas-Prat, 2014; Sánchez-Arcilla et al., 2016). In addition, SLR may increase overtopping of port breakwaters (Zviely et al., 2015; Sierra et al., 2016; Pillai et al., 2019; Contestabile et al., 2020; Maravelakis et al., 2021) or affect port operability by reducing the freeboard in berthing areas (Gracia et al., 2019; Hanson and Nicholls, 2020; Verschuur et al., 2020; Izaguirre et al., 2021; Jebbad et al., 2022). Moreover, SLR will increase water depths in ports and neighboring areas which, in turn, will modify wave propagation patterns and, therefore, will contribute to the aforementioned impacts on port operations caused by waves. It must be pointed out that these last impacts may be either negative or positive, i.e. they can worsen or improve port operability (Sánchez-Arcilla et al., 2016; Sierra et al., 2017). In addition, SLR can also have positive impacts on ports by reducing dredging maintenance costs or by enabling the port to receive larger vessels (Chhetri et al., 2016).

Although in the last years the number of studies tackling climate change impacts on harbors has increased significantly (Hanson et al., 2011; Becker et al., 2012; Ng et al., 2013; Nursey-Bray et al., 2013; Chhetri et al., 2015; Sánchez-Arcilla et al., 2016; Izaguirre et al., 2021), few of such studies have considered the combination of drivers (sea level rise and changes in storm surge and wave climate) contributing to such impacts, therefore underestimating resulting risk assessments. In addition, although there is some study on a global scale (Izaguirre et al., 2021), most are concentrated in one or a few ports and there is a gap in the literature on regional scale studies with a high level of detail.

Another aspect not traditionally addressed in the literature related to the impact of climate change on ports is the adoption of adaptation measures. Only in recent times there have been studies analyzing impacts and proposing adaptation measures, such as those of Yang et al. (2018); Ng et al. (2018); Sierra (2019); Portillo Juan et al. (2022) and Loza and Veloso-Gomes (2023).

The aim of the study is to assess changes in port operability associated to combined drivers that encompass SLR, storm surge and wave pattern variations induced by climatic change. The work focuses on the potential impacts of these drivers on two of the processes that may generate higher risks of disrupting port services: i) inner agitation generated by changes in wave storminess and alterations of wave patterns due to SLR, which may affect port operations (Rusu and Guedes Soares, 2013) and cannot exceed certain thresholds, which depend on the type of operation (mooring, loading or unloading) and cargo involved (López et al., 2015); ii) reduction of berthing structure freeboards due to SLR and modifications in storm surge patterns that can lead to temporary or permanent flooding of the docks (Gracia et al., 2019; Jebbad et al., 2022). In addition to analyzing the impact of climate change on port operability, adaptation measures have been proposed and a rough estimation of their cost and performance estimated. The study is developed for the Balearic Islands (NW Mediterranean), starting with an analysis at regional scale, identifying the harbours that may have an excess of agitation or insufficient berthing structure freeboard, which together increase risks or prevent port operations. Although the study focuses on ports of a specific region, the methodology here described is applicable to any port worldwide.

2 Site description and climate

The study area corresponds to the Balearic Islands (western Mediterranean Sea, from 38°38'N to 40°06'N and from 1°09'E to 4° 20'E). These islands form an archipelago (Figure 1) with four major islands (Mallorca, Menorca, Eivissa and Formentera) and several islets.

The Mediterranean Sea basin has been widely studied due to its vulnerability to SLR (Lorente et al., 2021) and other hazards, such as rogue waves (Cavaleri et al., 2012), erosion and flooding (Wolff et al., 2018), storm surges (Lin-Ye et al., 2020) or "Medicanes" (Mediterranean hurricanes), which are strong cyclonic systems (Milglietta and Rotunno, 2019; Kassis and Varlas, 2021). The potential impacts of climate change in Mediterranean coasts are specially worrying because 34% of the population lives in the coastal fringe in contrast to 10% worldwide (Luque et al., 2021). In addition, much of the Mediterranean coast is a high popular place of recreation, attracting millions of tourists every year (Juza and Tintoré, 2021).

This region is subjected to strong and increasing pressures such as natural hazards, tourism, navigation, pollution and overfishing (Visbeck, 2018; Ryabinin et al., 2019), which can be exacerbated by climate change effects, because the Mediterranean is a semi-enclosed and relatively small basin (Giorgi, 2006; Lionello and Scarascia, 2018). Additional environmental problems in this area include proliferation of harmful algal bloom episodes (Ferrante et al., 2013) and ocean acidification (Hilmi et al., 2014; Lacoue-Labarthe et al., 2016).

Regarding the marine forcings, the Balearic Islands coast is a microtidal environment with tidal ranges smaller than 25 cm (Orfila et al., 2005; Bonaduce et al., 2016), while storm surge reaches 25-30 cm at the coast (Agulles et al., 2021). On the other hand, the wave climate in this area is highly variable (Sánchez-Arcilla et al., 2008; Campins et al., 2011; Morales-Márquez et al., 2020) due to its complexity (orography, bathymetry, veering winds…) and semi-enclosed character (area with limited fetches because it is surrounded by coastal areas and other islands). Under mean conditions (usually between April and September) the regional winds are mild and due to the short fetches in the area, they generate short waves, with significant wave heights (Hs) between 0.1 and 1 m and peak wave periods (Tp) between 3 and 6 s (Alvarez-Ellacuria et al., 2011). The most energetic wave conditions (Hs up to 7 m and Tp up to 12 s) come from the north and are due to cyclonic activity in the Gulf of Lions, while in the southern coasts of the Balearic archipelago, waves propagating from SW (Hs up to 6 m) and SE (Hs up to 3 m) (Agulles et al., 2021) prevail. Nevertheless, when performing extreme analyses in the Mediterranean area, as pointed out by de Leo et al. (2021a), caution should be exercised with the values of Hs and Tp obtained, since they show a marked dependence on the time window considered.

With respect to future wave climate in the Mediterranean Sea, a relative decrease in wave energy is expected in general (Lionello and Sanna, 2005; Lionello et al., 2008; Marcos et al., 2011; Conte and Lionello, 2013), with some local increases. These projections are similar to the results of Casas-Prat and Sierra (2013) who found a decrease of Hs in large areas of the NW Mediterranean, with local increases in other places such as the Gulf of Genoa. Lionello and Giorgi (2007) and Casas-Prat and Sierra (2013) also found modifications of the seasonal wave distribution with greater median Hs in summer and lower in winter and different directional frequencies. In the same way, more recent studies on wave climate projections on the Spanish Mediterranean Coast show a decrease in the highest wave heights in the stormy season (November-March) but an increase in the calmer months (Lira-Loarca et al., 2021). Other authors such as Kapelonis et al. (2015) also obtained a general reduction of extreme events in the Mediterranean basin with slightly increased extreme activity in certain areas, while Bonaldo et al. (2020) found a similar pattern for the Adriatic Sea. More recent studies (Morim et al., 2018; de Leo et al., 2021b; Lira-Loarca and Besio, 2022) also found a decrease of the average Hs over the Mediterranean Sea. However, despite the fact that all projections indicate a general reduction in Hs, especially

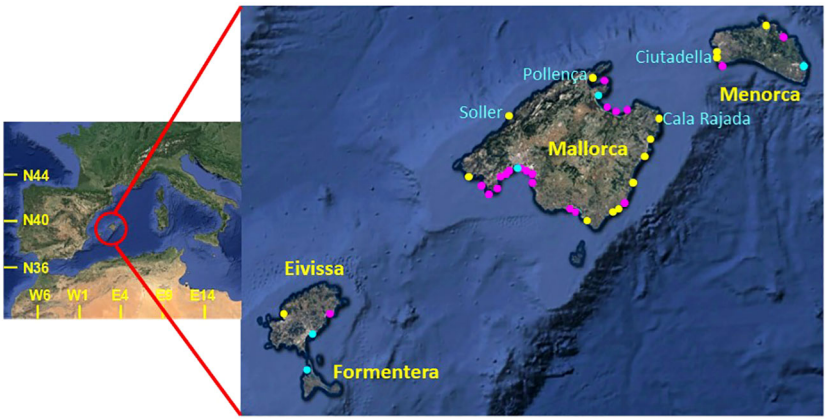

FIGURE 1
Geographic location of the Balearic Islands and the studied ports. Yellow: ports managed directly by regional authorities (PIB); magenta: ports under administrative concession; light blue: location of tidal gauges. The text in yellow indicates the names of the islands and in blue the name of the ports mentioned in the study.

towards the end of the century, a recent study in which wave hindcasting data from 41 years were analysed in different areas of the Mediterranean Sea showed an increase in the number and intensity of wave storm events over recent years (Amarouche et al., 2022).

Concerning storm surges, a number of studies have assessed its levels along Mediterranean coasts as a consequence of climate change (Marcos et al., 2011; Jordà et al., 2012; Conte and Lionello, 2013). Results showed no significant changes in extreme values due to storminess (Conte and Lionello, 2014; Lionello et al., 2017) and even a small decrease of the amplitude of storm surge along Mediterranean Sea coasts (Lionello et al., 2008; Marcos et al., 2011; Conte and Lionello, 2013). In the same way, Vousdoukas et al. (2016) projected, in general, minimal changes or even small decreases along European coastal areas South of 50°N.

In the Balearic Islands there are 5 commercial ports classified by Spanish Port System as "Ports of General Interest" which are managed by national authorities. In addition, there are 33 smaller ports administrated by regional authorities through a public body, *Ports de les Illes Balears* (PIB). From these 33 ports, 14 are managed directly by PIB and 19 are operated by private entities under administrative concession. In 32 of the 33 ports there are facilities for leisure craft and 8 of them are also the base for fishing activities, while only 2 ports have passenger traffic and ferries. These 33 regional ports are the object of the presented analysis.

3 Materials and methods

3.1 Data sources

In its 5th Assessment Report (AR5), the Intergovernmental Panel on Climate Change (IPCC, 2013) proposed four future scenarios depending on the evolution of the emissions until the end of the 21st century. Regarding SLR, each scenario has a central estimate and two confidence bands. IPCC (2013) estimates of global SLR at year 2100 range between 0.52 and 0.98 m (5% to 95% confidence interval) with respect to the 1986-2005 period, for the highest emissions RCP8.5 scenario. Nevertheless, according to IPCC (2013), SLR has a 33% probability to lie outside such interval, due to uncertainty induced by the potential collapse of the Antarctica ice sheet areas. Other studies project higher values for 2100: up to 1.86 m (Jevrejeva et al., 2012; Mori et al., 2013) or even up to 2m (Rahmstorf, 2007), which are physically feasible although with a probability of occurrence smaller than 5% (Jevrejeva et al., 2014). Moreover, AR5 projections (IPCC, 2013) indicate that SLR in the Mediterranean Sea will be slightly lower than the global SLR average. This is because sea level is expected to decrease in semi-enclosed and inland seas (e.g., Mediterranean Sea, Black Sea) due to the greater rates of evaporation (Yin et al., 2010). Thus, in the NW Mediterranean, for the RCP8.5 scenario SLR is projected to be in the range 0.40 to 0.85 m (90% confidence interval, Sánchez-Arcilla et al., 2016) by 2100. In this work, two of such scenarios have been considered, one intermediate (RCP4.5) and other pessimistic (RCP8.5). For scenario RCP4.5 the central values of SLR were taken into account, while for RCP8.5 the upper band was selected. In this way, the assumed magnitudes of SLR correspond to high probability values (RCP4.5) and the worst projected (RCP8.5) estimate. In addition, for each scenario, two-time horizons were considered: a medium term one (2045) and a long term one (2100). The values of SLR used in the study are consequently: 18 cm (RCP4.5, 2045), 25 cm (RCP8.5, 2045), 47 cm (RCP4.5, 2100) and 88 cm (RCP8.5, 2100).

The reason for using the AR5 projections instead of those of the 6th Assessment Report or AR6 (IPCC, 2021), is that most of the work was carried out before the latter was released. Nevertheless, looking at the NASA Sea Level Projection Tool for the AR6 (https://sealevel.nasa.gov/ipcc-ar6-sea-level-projection-tool), the average values of SLR for the Balearic Islands in the equivalent scenarios are the following: 20 cm (SSP2-4.5, 2045), 23 cm (SSP5-8.5, 2045), 58 cm (SSP2-4.5, 2100) and 91 cm (SSP5-8.5, 2100). It can be verified that in three of the four cases, the values are very similar, with differences of 3 cm or less. Therefore, the risk analysis carried out for the studied ports would provide similar results regardless of the AR applied. Only in the intermediate scenario (RCP4.5 or SSP2-4.5) and for the 2100 horizon, there is a significant difference between AR5 and AR6 SLR values (47 cm *vs.* 58 cm). The uncertainties in these projections, together with those in the formulations to calculate risk variables, as well as the fact that the SLR value considered in such intermediate scenario is within the range foreseen in AR6 (46 to 92 cm) make the obtained results a reasonable estimate for climatic impacts in the considered horizons.

The performed analysis considers SLR together with variations in mean sea level due to tides and storm surges. With this aim, data from the tidal gauge network managed by the Spanish Harbour Authority (Puertos del Estado) were gathered. This network has 5 tidal gauges in the Balearic Islands (see Figure 1) and in the webpage https://www.puertos.es/en-us/oceanografia/Pages/portus.aspx, the corresponding reports for each tidal gauge can be found, such as EPPE (2019). For each harbour, the 99.9 percentile of sea level corresponding to the closest tidal gauge was assumed. This percentile was selected because it defines the operative level window, according to the recommendations of Puertos del Estado (EPPE, 2012). In addition, the database of marine climatic projections in Spain developed by the *Instituto de Hidráulica Ambiental de la Universidad de Cantabria* (IHC) was used to get data on wave climate and changes in storm surges for the selected scenarios and time horizons.

Different global climate models (GCMs) used in CMIP5 (Taylor et al., 2012) were used as forcings to develop this database. Subsequently, downscaling was performed with regional climate models (RCMs), coming from the CORDEX program: EURO-CORDEX (Kotlarski et al., 2014), which covers the European domain and focuses on atmospheric modeling, and MED-CORDEX (Ruti et al., 2016), which covers the Mediterranean and considers coupled atmospheric-ocean models. RCMs have been used for meteorological wave and storm surge climate projections.

The WaveWatch III numerical model (WW3; version 4.18; Tolman, 2002) was used to calculate the wave projections. In order to validate the applied dynamic downscaling methodology, the results obtained during the historical reference period 1985-2005 were compared with wave buoy data. For this purpose, atmospheric

variables from the ERA-5 reanalysis database (Dee et al., 2011) have been used as a forcing of the WW3 model. The obtained wave data are available in hourly time series (with only Hs, Tp and mean direction) at points separated by 0.08°. To obtain the wave data used in the study, 9 climate models were utilized for the present situation and 6 for the four future scenarios. With these data, an ensemble was made to produce more representative wave projections.

It should be noted that to perform a detailed analysis about changes in wave climate, this analysis should be done on the spectra (which are not available in this case) and not on integral quantities (Portilla-Yandun et al., 2016; Echevarria et al., 2019; Shimura and Mori, 2019; Lobeto et al., 2021b), since there may be a transfer of energy between frequencies and/or directions. Thus, for example, Lira-Loarca and Besio (2022), analyzing data from the Mediterranean Sea, found that although the average Hs decreases, there are increases in other less energetic frequencies and directions leading to a projected change from unimodal to bimodal/multimodal wave climate in many locations, which may have strong impacts on coastal and port areas.

The dynamic projections of the meteorological component of the sea level (or meteorological tide) have been simulated using the ocean circulation model ROMS, version 3.5 (Regional Ocean Modeling System, Shchepetkin and McWilliams, 2005). The dynamic downscaling methodology used for the storm surge climate projections has been validated using *in situ* measurements from the Puertos del Estado tidal gauges. A comprehensive description of the database generation and validation process can be found in Ramírez et al. (2019).

To take into account changes in storm surges, for each port the data corresponding to the closest point were used. In addition, assuming that the effect of climate change on astronomical tide is negligible in the Mediterranean basin (Lionello et al., 2005; Marcos et al., 2009; Tsimplis and Shaw, 2010; Conte and Lionello, 2014), in this study the present astronomical tidal levels were considered constant along the 21st century.

To extract time series of wave data from the periods 2026-2045 and 2081-2100, 10 control points were selected from this database and for the two climatic scenarios considered (RCP4.5 and RCP8.5). The 10 points were chosen to cover the locations of all considered ports with the minimum number of points possible to limit the amount of numerical simulations to be carried out. These points are shown in Figure 2, as well as the grids used to carry out the numerical simulations to propagate wave fields.

Finally, bathymetric information was obtained from the General Bathymetric Charts of Ocean (GEBCO) datasets (http://www.gebco.net), which have a resolution of 30 arc-second grid. In the areas close to the ports (up to depths of about 100 m), this information was complemented by high-resolution bathymetric information provided by the Ports Authority, PIB, which also supplied topographical data on berth facilities and port land areas.

3.2 Methodology

The impacts of climate change presented in this work are port agitation and inoperability of berthing areas due to insufficient freeboard. Due to the huge amount of numerical simulations to be carried out, the study of wave agitation was limited to the 14 ports that are directly managed by PIB. However, the analysis of inoperability for berthing areas due to freeboard reduction covered the 33 ports of the region.

For the study of agitation within the ports, two numerical wave models were used. The first one was the SWAN code (Booij et al., 1999; Ris et al., 1999), where offshore wave conditions were given by the projections described in the previous section at all selected points (see Figure 2). The model was implemented with two nested grids, with resolutions of 100x100 m and 10x10 m, respectively, and it was used to propagate wave conditions from the offshore to the port entrances. The bathymetry provided by GEBCO is rather coarse, so it has been necessary to interpolate it in the first domain. In the areas closer to the coast (up to depths of about 100 m), information from nautical charts has been taken into account to improve this interpolation and to match the coarse bathymetry with that of the nested grid. Since in this open area, shoaling and refraction are the prevailing processes, the SWAN code is appropriate to simulate wave propagation in these outer domains.

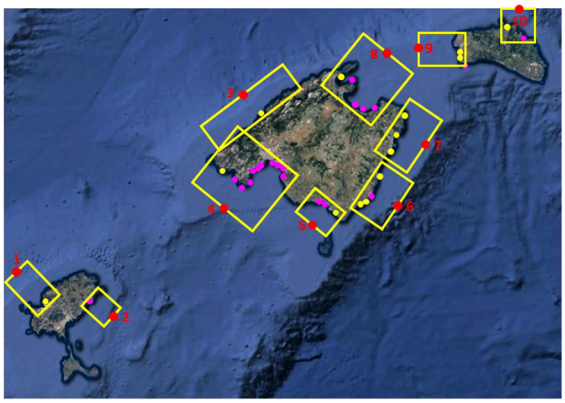

FIGURE 2
Location of the points (in red) from which projected wave information was extracted and the numerical grids used to propagate such wave information towards the analysed ports.

To simulate agitation within the harbours, diffraction and reflection are also important, so another type of model must be used. The Boussinesq-type (BT) models have been widely used to analyse wave propagation in port environments (e.g. Woo and Liu, 2004; Belloti, 2007; Belloti and Franco, 2011; Thotagamuwage and Pattiaratchi, 2014; Zheng et al., 2020; Malej et al., 2021). For this reason, in this case a BT model (LIMPORT, developed by the research team, Sierra et al., 1988) was used with a variable spatial resolution between 3x3 m and 5x5 m, depending on port size. This model had been used in previous works (González-Marco et al., 2008; Casas-Prat and Sierra, 2010; Casas-Prat and Sierra, 2012; Sierra et al., 2015; Sierra et al., 2017) giving good results. The model configuration could not be validated in the study area due to the lack of simultaneous wave data inside and outside the studied harbours. Nevertheless, this model was validated in other Mediterranean areas in previous works (Sierra et al., 2017). Since the paper analyses differences between future and present conditions rather than local spatial variations in the Hs fields, this approach should capture the temporal variations, as it has been shown for other nearby harbour domains where the validation was carried out. Moreover, the simulations with the BT model are performed using identical arrangements in domains, discretisations and boundary condition type for present and future conditions, so no bias in the results are expected. Therefore, for comparative purposes as carried out in this work, the obtained results can be considered representative of changes in wave agitation due to climate change (SLR and different wave conditions) within the studied ports.

Since at each point, data from different models were available (9 models for present conditions and 6 models for future scenarios), the direct propagation of the whole 20-year time series for each model and scenario was unfeasible. Instead of this, a lumped wave characterization was applied, grouping the wave data in 22.5° directional sectors (N, NNE, NE, ENE…) and in 1 meter Hs bins (0-1, 1-2, 2-3,… m). The next step consisted of determining the frequency of occurrence of each direction and range of Hs for every model and scenario and performing an ensemble (averaging these frequencies of occurrence) for each scenario. The minimum frequency of occurrence considered was 0.0001%. Therefore, the number of simulations depends on the port and the scenario, since in each port this frequency changes and the number of directions with incidence on the port also change. Most of the ports are located in bays and in very sheltered areas, so the directions of incidence on them are limited, varying from only 1 for the Pollença port to 6 for the Ciutadella port. The total number of simulations (considering all ports) for each scenario was 285 (RCP4.5) and 267 (RCP8.5) for horizon 2045, while for horizon 2100 it was 277 (RCP4.5) and 259 (RCP8.5).

Moreover, for every Hs and direction, the central values of the bins were used to execute the simulations. The value of the wave period was obtained, following the recommendations of the Spanish Harbour Authority (EPPE, 2021), using the equation:

$$T_p = aH_s^b$$

being Tp the wave period and *a, b* two coefficients fitted to each wave data projection set. Correlation coefficients have been measured between the periods provided in the time series and those calculated using the formula. Depending on the point and the scenario considered, the correlation coefficient varies between 0.57 and 0.72.

The obtained combinations of direction, Hs and Tp were used as boundary conditions in the SWAN model which, in turn, provided the boundary conditions for the BT model. Running this last model, Hs was obtained at all the grid points within the 14 studied harbours. From here, considering the limits fixed by the Spanish Recommendations for Maritime Works ROM 3.1-99 (EPPE, 2000), the following thresholds were considered to delineate safe harbour operation spaces:

- Yachts and leisure crafts: Hs = 0.4 m and 0.2 m for waves longitudinal or transversal to the berth respectively.
- Fishing boats: Hs = 0.6 m and = 0.4 m for waves longitudinal or transversal to the berth respectively.
- Ferries and cruises: Hs = 0.5 m and 0.3 m for waves longitudinal or transversal to the berth respectively.

When the obtained Hs at a berthing area exceeds the aforementioned thresholds, the berthing area becomes inoperative for these specific wave conditions. The sum of frequencies from all the wave conditions exceeding the threshold at every berthing area gives its total inoperability, for each of the four studied scenarios. This total frequency can be transformed in average annual hours of inoperability by multiplying it by 365 (days) and 24 (hours).

Since the aforementioned ROM 3.1-99 (EPPE, 2000) set as maximum inoperability time 200 hours/year, a risk level was assigned to each berthing area depending on the number of inoperability hours, according to the following Table 1, discussed with the port stakeholders.

Finally, a global risk level was assigned to every port, consisting of the maximum risk level reached by any of the berthing areas within the port because, although such level of inoperability only affects part of the port, this means that the facility requires adaptation measures to deal with such levels of risk.

On the other hand, to determine if a berthing structure becomes inoperative due to insufficient freeboard, for every scenario and

TABLE 1 Risk levels due to port agitation, based on the number of hours per year (*t*) in which the indicated thresholds are exceeded.

Risk level	Risk	Hours/year of inoperability
0	Without risk	t< 200
1	Very low	200 ≤ t< 240
2	Low	240 ≤ t< 280
3	Medium	280 ≤ t< 320
4	High	320 ≤ t< 360
5	Very high	t ≥ 360

season considered, the values of SLR and variation of storm surge at each port are added to the 99.9 percentile of present levels due to astronomic tide and storm surge. The final level is compared to the topographic elevation of berthing structures to obtain the final freeboard, as shown in Figure 3. The minimum freeboard necessary for berthing structures to be operative depends on the type of boats operating there. These freeboards, according to Port expertise, are: 0.15 m for leisure crafts, 0.5 m for fishing boats and 1.5 m for commercial vessels (EPPE, 2012). If the final freeboard is smaller than the corresponding minimum values, the berthing structure remains inoperative and if the final freeboard is negative, this means that besides being inoperative, sometimes it will be flooded.

A risk scale was established for every port based on the percentage of berthing structures that became inoperative for each scenario and horizon. It must be stressed that the berthing structures were divided into docks and piers, because the adaptation measures for both are different. In addition, some piers were floating structures, which means that they were easily adaptable to SLR and, as a consequence, they would not be affected by climate change. Depending on the percentage of docks and piers affected by inoperability and flooding, the following risk scale, discussed with port stakeholders, was defined (Table 2).

Considering the scale presented in Table 2, for each port two risk levels due to inoperability of berthing structures were obtained, one corresponding to docks and the other one to piers.

After estimating the risk levels of inoperability due to excessive agitation and insufficient freeboard, adaptation measures should be proposed. In the case of excessive future agitation within a harbor, adaptation measures should be specific for each port but, in general terms, they should consist of modifying port layout by enlarging breakwaters or constructing additional structures. Since the volume of the works will depend on the necessary length of new (or enlarged) structures, as well as the water depth at which they will be located, the adaptation cost of the studied ports to the potential increase of agitation due to climate change cannot be assessed at this stage.

The adaptation measures to solve the problems resulting from insufficient freeboard depend on the type of berthing structure. In the case of piers, the more sustainable measure consists of the substitution of fixed piers by floating ones. In the case of docks, to prevent their inoperability, the easiest measure is the increase of their elevation, by adding a layer of concrete or units suitable for marine environments.

As in the case of agitation, the assessment of the adaptation costs to the inoperability of berthing structures due to climate change requires individual studies for each port. Nevertheless, based on recent projects, a rough estimate of the unitary costs (in current monetary units) may be established. In the case of docks, the cost is around 250 €/m^3 of additional dock (due to its elevation). In the case of piers, the costs are 430 € for the removal of a pile, 120 €/m^3 for the removal of the fixed pier, and 900 €/m^2 of floating pier once placed.

We assume that the average width of the piers (both fixed and floating) is 3 m and the average separation between piles is 6 m. In addition, since the thickness of a fixed pier varies between 0.3 m and 0.8 m and the information about this parameter is not available for every pier, we considered an average thickness of 0.5 m. Finally, a dock elevation has been assumed for each scenario to keep operability at current levels. To this aim, the minimum necessary values (equal to the SLR rounded to multiples of 10 cm) are: 20 cm (RCP4.5 – 2045), 30 cm (RCP8.5 – 2045), 50 cm (RCP4.5 – 2100) and 90 cm (RCP8.5 – 2100). Note that these values represent a lower bound of the adaptation costs since they only balance the SLR. Probably, port authorities would adopt greater elevation values to prepare docks for future level rises.

4 Results

4.1 Wave agitation

For comparative purposes, the annual average Hs was computed at each point of the port grids for the present situation and the four future scenarios. This was done (for each scenario) by multiplying the Hs obtained at each node in each numerical simulation by the frequency of presentation of the wave conditions simulated and making the addition of the values corresponding to all simulations at each node. It must be pointed out that, in future scenarios, the water depth at each grid point was increased by the corresponding value of climatic SLR.

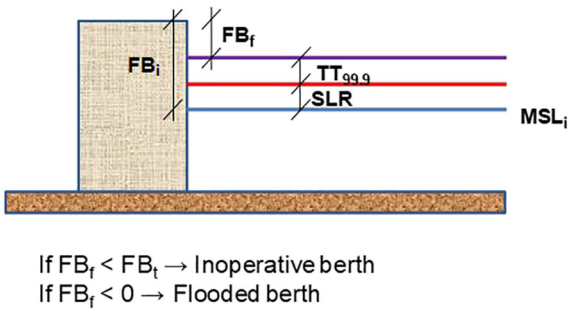

FIGURE 3
Sketch showing the inoperability or flooding of berthing structures. FBi, initial freeboard; FBf, final freeboard; FBt, threshold freeboard; MSLi, initial mean sea level; SLR, sea level rise due to climate change; TT99.9, 99.9 percentile of the level resulting from combining tide and storm surge (including changes in storm surge due to climate change).

TABLE 2 Risk levels due to insufficient freeboard, based on the percentage (*n*) of inoperative berthing structures.

Risk level	Risk	% Inoperative berths
0	Without risk	0
1	Very low	0< n ≤ 20
2	Low	20< n ≤ 40
3	Medium	40< n ≤ 60
4	High	60< n ≤ 80
5	Very high	t > 80

Once the annual average Hs was determined at each port point, the differences between future and present scenarios were assessed by subtracting the future from the present Hs. Therefore, positive values indicate a future increase of the annual average Hs, while negative values mean a future decrease of such parameter. An example of these results is presented in Figures 4 and 5, where these difference Hs maps are plotted for the ports of Cala Rajada and outer Ciutadella, respectively. In both cases, since the average annual Hs were small (0.75 and 0.82 m in deep water, significantly smaller within the ports), the variations of this parameter in absolute terms were very low (only a few cm). Nevertheless, both cases present different behaviours that will be analysed more in detail in the next section.

In addition, as described in the Methodology, at each berthing area of the studied ports, the time in which the threshold values of Hs were exceeded was computed and, taking into account this time, for every scenario a risk level was assigned to every port according to Table 1. For each scenario, the number of ports that have associated a certain level of risk is represented in Figure 6. This number barely changes in the different scenarios, as could be expected from observation of Figures 4 and 5. Notice that, in the present situation, two ports had already a very high risk of excessive agitation, 10 had no risk, 1 very low and 1 low risks.

4.2 Inoperability due to insufficient freeboard

To illustrate the impact of SLR on dock and pier inoperability due to insufficient freeboard, Figure 7 shows the evolution, under future scenarios, of Soller harbour, a port in which most of the piers are floating. Such type of piers can be easily adapted to SLR, so that they remain operative whatever the value of SLR. In this and next figures, we distinguish between structures with insufficient freeboard (marked in yellow) and those that eventually (depending on the conditions of tide and storm surge) can be flooded (marked in red). Notice that in the port shown in Figure 7, besides the floating piers, most of the docks have enough freeboard for not losing operability due to SLR, being an example of a port barely affected by the climatic SLR. As a consequence, its level of risk is not high in the different scenarios being, in the case of docks, very low in 2045 (for both climatic scenarios) and medium in 2100 (also for both scenarios). In the case of piers, for both scenarios, the levels of risk are very low in 2045 and low in 2100.

Figure 8 also shows the evolution of the inoperability of berthing structures with SLR in another illustrative port. In this case (Pollença harbor), all the piers and docks are fixed and, therefore, they cannot follow the SLR as in the case of floating piers. As a consequence, most of the berthing structures are affected and all of them become inoperative by 2100. In the case of docks, the risk is low (RCP 4.5) or medium (RCP8.5) in 2045 and very high

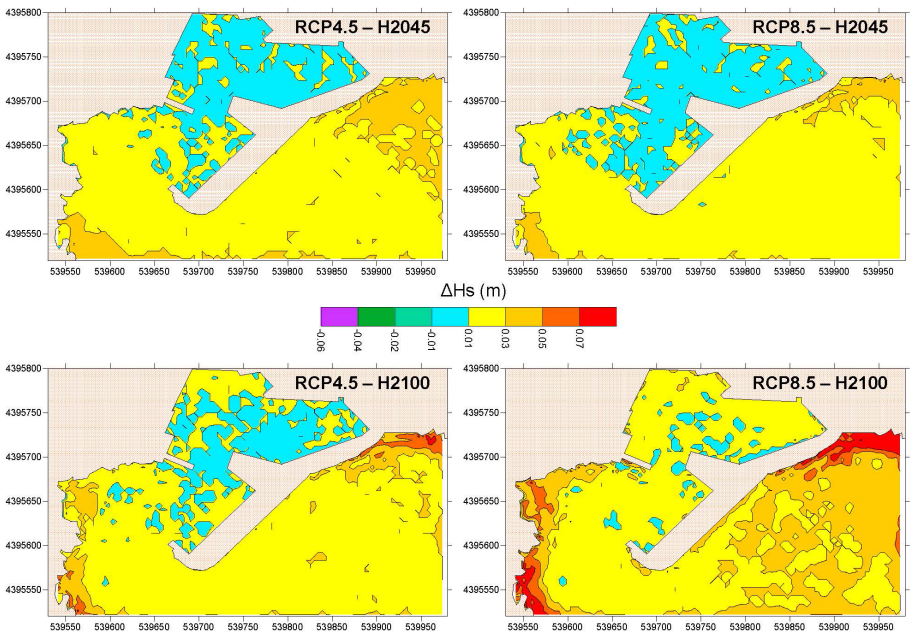

FIGURE 4
Port of Cala Rajada. Differences between future and present annual average Hs. The values on both axes indicate UTM coordinates.

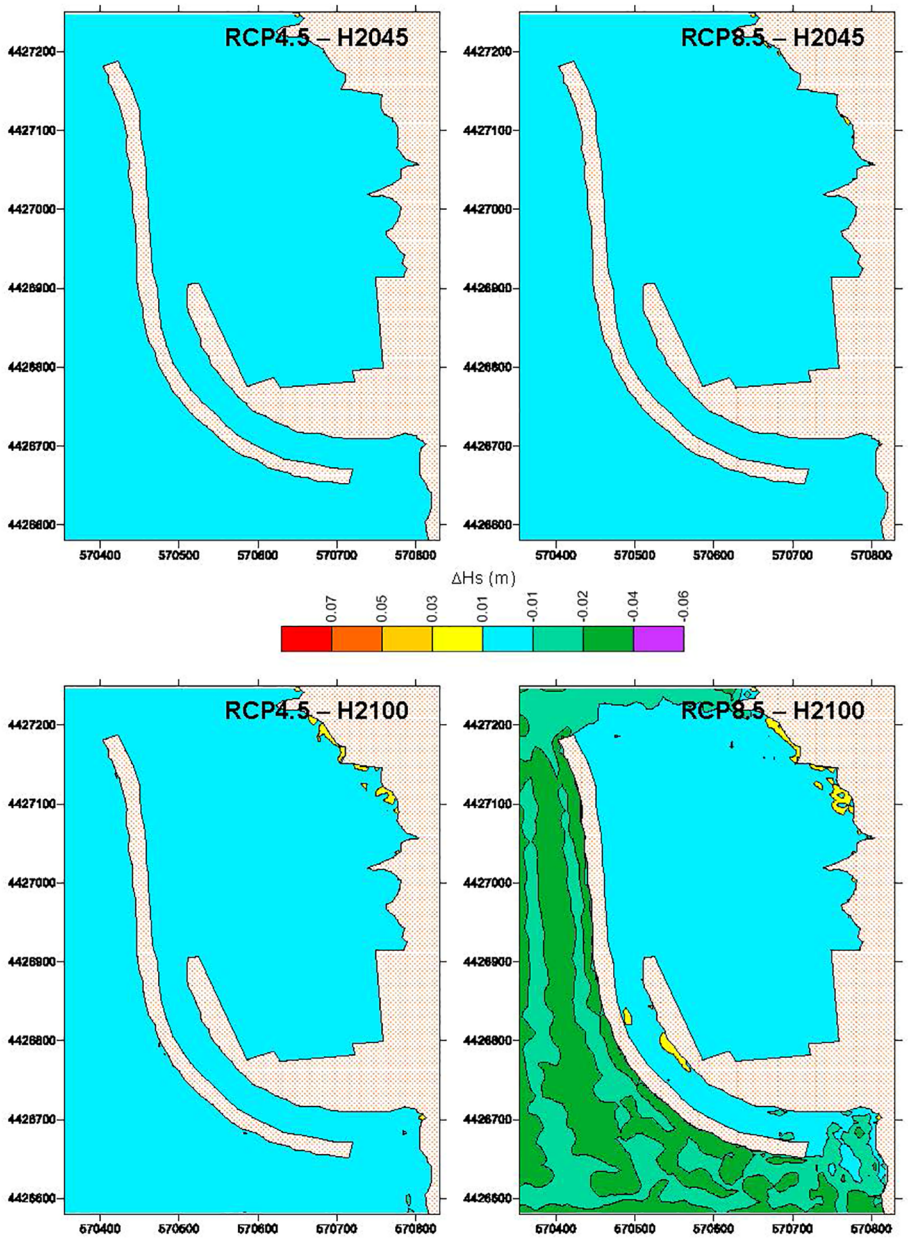

FIGURE 5
Outer port of Ciutadella. Differences between future and present annual average Hs. The values on both axes indicate UTM coordinates.

in 2100 (for both scenarios). In the case of piers, the risk is medium (RCP4.5) or high (RCP8.5) in 2045 and also very high in 2100 for both climatic scenarios.

In Figure 9 the distribution of risk levels due to insufficient freeboard in docks under different scenarios is shown. In this figure, a clear increase of risk levels associated to greater SLR can be observed. In particular, in horizon 2100 for both scenarios, such an increase becomes clearly apparent, with 17 (RCP4.5) and 29 (RCP8.5) ports attaining the maximum level of risk.

In Figure 10 the same distribution as in the previous figure is shown, but corresponding to piers instead of docks. Here, the shift from low levels of risk to higher values is also observed, but in a less noticeable way. This is because many harbours have floating piers, which are not affected by climatic SLR.

4.3 Adaptation measures

As indicated in the Methodology section, the adaptation measures in case of excessive future agitation must be very particular to each port and will consist of the construction of new structures or the modification of existing ones. Since the magnitude of the works will be very case specific, their cost cannot be assessed. Nevertheless, there is already a project to solve the current excessive

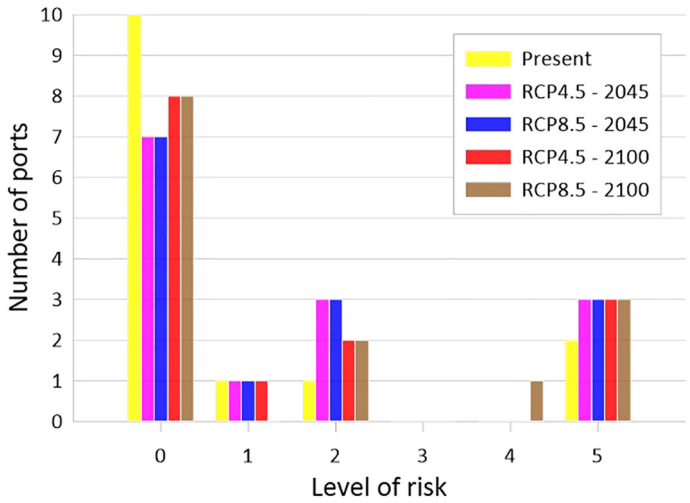

FIGURE 6
Number of ports corresponding to the different levels of risk due to excessive agitation for the present situation and the future scenarios.

agitation in one of the ports with such problems (level risk of 5 in the present situation) and the estimated budget for such project is around 6 million euros in current monetary units. Taking into account this, a rough estimation for the adaptation to excessive agitation in the future scenarios should be about 5 times such cost and, therefore, would amount to a value of around 30 million euros (in current monetary units).

The adaptation measures for insufficient freeboard in the berthing structures and their preliminary estimated unitary cost were described in the Methodology section. The total cost will depend on the total length of the structures affected and to be replaced or upgraded. The total length of docks in the 33 studied ports is 32.2 Km and the length of piers is 15.2 Km. The total inoperative length of docks and piers under each scenario is summarized in Table 3.

Taking into account the magnitudes of dock elevation (and their cost) indicated in the Methodology section, and the costs of substitution of piers, a rough estimation of the adaptation costs to inoperability of berthing structures is obtained and summarized in Table 4.

5 Discussion

Concerning agitation, from the analysis of Figures 4–6, it may be concluded that agitation patterns are not significantly modified

FIGURE 7
Evolution of the inoperability of berthing structures at the port of Soller in future scenarios. Yellow: structures with insufficient freeboard; red: structures that can be flooded. Note that most of the piers remain operative because they are floating piers.

FIGURE 8
Evolution of the inoperability of berthing structures at the port of Pollença in future scenarios. Yellow: structures with insufficient freeboard; red: structures that can be flooded. Note that all the piers are inoperative in 2100 because they are fixed piers.

in the studied Mediterranean ports due to climate change. The study of Figure 4 indicates that the variations of average annual Hs (within the port) in the different scenarios, with respect to the present situation, are small in absolute terms. Nevertheless, in this case, a slight but progressive increase of the average annual Hs with SLR can be observed, specifically in horizon 2100, where SLR is 47 cm (RCP4.5) or 88 cm (RCP8.5). This increase can be attributed to the fact that, in this port (Cala Rajada), representative of limited depth harbors, the increases of water depth associated to SLR represent significant changes, in relative terms, of the total water depth, since at the present situation, these water depths vary between 1 m and 5 m. As a consequence, since water depths increase in a significant percentage under future scenarios, the wave lengths also increase. As pointed out by Sierra et al. (2015); Sierra et al. (2017), greater wave lengths give rise to greater diffraction coefficients and, therefore, waves penetrate more easily within the port, producing greater Hs. Therefore, in ports with reduced water depths as Cala Rajada, the enhanced diffraction could generate greater Hs within the harbors under future scenarios, in particular in 2100. Nevertheless, such increases may not be large enough to lead to a significant increase of risk levels for the ports studied.

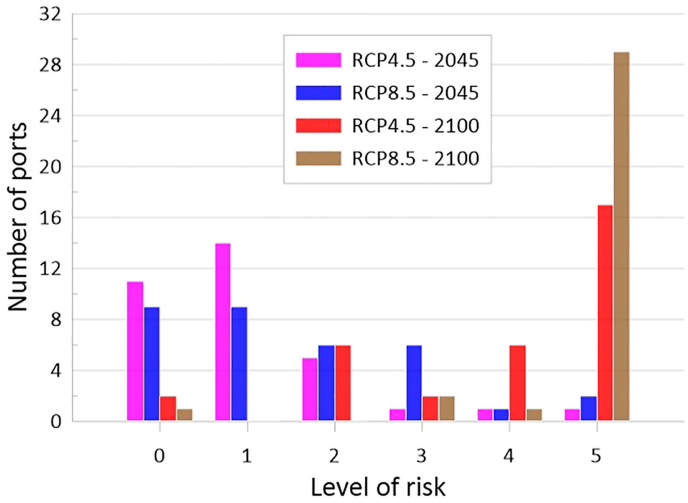

FIGURE 9
Number de ports for each level of risk due to inoperability of the docks under the two horizons and scenarios considered.

10.3389/fmars.2023.1124763

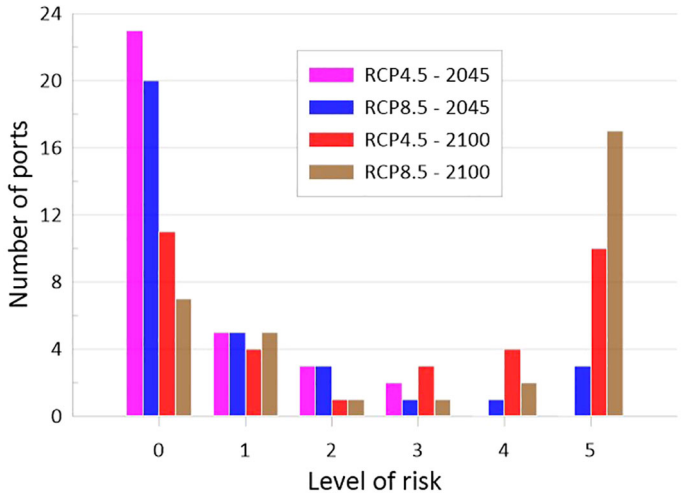

FIGURE 10
Number de ports for each level of risk due to inoperability of the piers under the two horizons and scenarios considered.

Another interesting feature observed in Figure 4 is the progressive increase of Hs with SLR in coastal areas surrounding the port. This is because the deeper waters associated to climatic SLR result in waves breaking closer to the current shoreline and with greater Hs values. Finally, the variation in Hs observed outside the port may be attributed to changes in shoaling and refraction patterns.

On the contrary, Figure 5 illustrates a port with a very different behavior. Hs variations within the port under future scenarios are negligible in spite of the increases of water depth. This is because this port currently has greater depths (between 10 m and 19 m) than in the previous case, so that SLR represents small relative changes of the water depth and, therefore, its effect on the wave lengths and diffraction coefficients is almost negligible. The only observed variations (reduction of average Hs) outside the port in scenario RCP8.5 in 2100 can be attributed to changes in shoaling and refraction patterns and also in reflections on the vertical breakwater that provides shelter to the port.

The analysis of how risk levels change under different scenarios (Figure 6) indicates that the variation in such risk levels is not significant. Note that most of the ports do not present risks associated with excessive agitation, being 10 (71.4%) in present conditions and 8 (57.1%) in both 2100 scenarios and 7 (50%) in both 2045 scenarios. This is because, as indicated above, most of the ports are located within natural bays that offer a very good shelter against wave action.

Besides the changes in water depth, the main factor contributing to port agitation is the mean wave climate, i.e. the distribution of Hs and wave directions. To analyze the influence of this factor at each selected climate point (see Figure 2), the variations of Hs (average annual and percentile 99.9) and direction are summarized in Tables 5, 6.

Data collected in Table 5 indicate a general trend with a very slight decrease of the average Hs (in the wave climate control points) in all future scenarios, although in RCP8.5 – 2045 four points do not show changes in Hs and one has an increase of 1 cm. This last scenario presents the smaller variations with respect to the current situation (changes between -2 cm and 1 cm). The other 2045 scenario presents a small range of Hs decrease (between -3 cm and -1 cm). On the contrary, in 2100, average Hs reductions are greater, ranging from -4 cm to -2 cm (RCP4.5) and from -7 cm to -3 cm (RCP8.5). Regarding the percentile 99.9 of Hs, with few exceptions, in most of the points there is also a decrease in the wave height. This reduction is greater than for the average Hs. In particular, for 2100, since all points show a reduction of the extreme Hs between 8 and 19 cm in RCP8.5 and between 2 and 10 cm in RCP4.5 (with the exception of one point where there is a positive variation of 1 cm). In 2045 the variations are smaller in RCP8.5,

TABLE 3 Total length (in Km) and percentage of berthing structures inoperable in the studied ports for every future scenario.

Scenario	Docks		Piers		Total	
	Length	%	Length	%	Length	%
RCP4.5 - 2045	3.48	10.8	1.49	9.8	4.97	10.5
RCP8.5 – 2045	7.19	22.3	2.52	16.6	9.71	20.5
RCP4.5 – 2100	20.82	64.6	6.28	41.4	27.10	57.1
RCP8.5 – 2100	29.16	90.4	10.31	67.9	39.47	83.2

TABLE 4 Total adaptation costs (in M€ and current monetary units) of the berthing infrastructures due to insufficient freeboard.

Item	Scenario			
	RCP4.5 - 2045	RCP8.5 - 2045	RCP4.5 - 2100	RCP8.5 - 2100
Dock elevation	1.91	5.68	27.52	70.67
Piles removal	0.24	0.38	0.92	1.50
Piers removal	0.27	0.45	1.13	1.86
Floating piers	4.03	6.80	16.96	27.84
Total costs	6.45	13.33	46.53	101.86

with reductions between 1 and 6 cm (except in three points where the changes range between 0 and 3 cm). In RCP4.5, the extreme Hs is reduced between 1 and 16 cm (except in two points with increments of 1 and 3 cm).

Regarding wave directions (Table 6), variations are also small in both 2045 scenarios, with values between -4.5° and 5.5° (RCP4.5) or -3.4° and 3.9° (RCP8.5), where the positive (negative) values indicate clockwise (counter clockwise) rotation. In 2100, changes in mean wave direction are greater, ranging from -4.8° to 7.3° (RCP4.5) or from -10.0° to 11.4° (RCP8.5).

In all cases the changes in average Hs and mean direction in the wave climate control points are quite small, so they will hardly generate significant changes in wave agitation within the harbors. In the case of extreme Hs (percentile 99.9) further reductions are projected in future scenarios, although it should be mentioned that these values have a very low frequency of occurrence (a few hours per year), so their contribution to the average annual agitation has a lower weight. Therefore, the small variations in risk levels due to excessive agitation in port berthing areas must be attributed to changes in wave propagation patterns associated to deeper waters because of climatic SLR. Such deeper waters modify shoaling, refraction, diffraction and reflection processes which, in turn, transform the spatial distribution of Hs within the ports. This is confirmed by the fact that the current situation is the one with most ports presenting zero agitation risk (10) and the least with very high risk (2), despite having greater Hs (in the wave climate control points) than in future scenarios (see Table 5). Ultimately, SLR contributes more to changes in port agitation in future scenarios than the projected variations in wave mean climate, which are very small as shown in Tables 5 and 6.

With respect to inoperability of berthing structures, there is an obvious direct relationship between SLR and the decrease of operability of such structures, although the results are different for docks and piers. Docks in the studied ports are fixed structures, so they cannot follow the SLR and their freeboard decreases with time and, therefore, they are more sensitive to variations of sea level.

On the other hand, piers may be fixed or floating. The first behave as the docks and they are more affected by SLR (see Figure 8), unlike the floating ones that may follow the sea level oscillations and do not become inoperative due to SLR (see Figure 7). For this reason, the shift to higher levels of risk due to SLR is more noticeable in the case of docks (Figure 9) than in the case of piers (Figure 10).

It must be pointed out that the main contributions to the reduction of berthing structure freeboards are the climatic SLR together with the contribution of tides and storm surges. Variations in storm surge have been assessed at each port for all the future scenarios, as indicated in the Methodology section, and represent a

TABLE 5 Variation of average annual Hs and 99.9th percentile of Hs (both in meters) at each selected control point (see Figure 2) in future scenarios with respect to present conditions.

Point	RCP4.5 - 2045		RCP8.5 - 2045		RCP4.5 -2100		RCP8.5 - 2100	
	ΔHs_{av}	$\Delta Hs_{99.9}$	ΔHs_{av}	$\Delta Hs_{99.9}$	ΔHs_{av}	$\Delta Hs_{99.9}$	ΔHs_{av}	$\Delta Hs_{99.9}$
1	-0.03	-0.11	-0.02	-0.02	-0.04	-0.10	-0.07	-0.19
2	-0.01	-0.01	0.00	-0.04	-0.02	-0.05	-0.03	-0.08
3	-0.03	-0.11	-0.01	-0.01	-0.04	-0.06	-0.06	-0.14
4	-0.02	0.03	-0.02	-0.05	-0.03	-0.03	-0.05	-0.17
5	-0.02	0.01	-0.01	-0.05	-0.03	-0.05	-0.05	-0.17
6	-0.02	-0.01	-0.01	0.00	-0.03	-0.02	-0.04	-0.13
7	-0.02	-0.07	0.00	0.02	-0.03	0.01	-0.04	-0.14
8	-0.01	-0.13	0.00	-0.06	-0.02	-0.07	-0.04	-0.19
9	-0.02	-0.16	0.00	-0.02	-0.03	-0.03	-0.06	-0.16
10	-0.01	-0.11	0.01	0.03	-0.03	-0.08	-0.05	-0.14

TABLE 6 Variation of average direction (in degrees) at each selected control point (see Figure 2) in future scenarios with respect to present conditions. Positive (negative) values of direction change indicate clockwise (counterclockwise) rotation.

Point	RCP4.5 - 2045	RCP8.5 - 2045	RCP4.5 -2100	RCP8.5 - 2100
1	3.9	3.9	4.1	7.3
2	-1.0	-1,5	-0.7	-0.8
3	3.7	3.3	3.8	6.2
4	-4.5	-3.3	-4,8	-10.0
5	-4.2	-3.4	-4.5	-9.0
6	-2.9	-3.0	-2.9	-5.6
7	-2.2	-2.4	-2.0	-2.9
8	3.4	2.5	4.3	6.8
9	5.5	3.3	7.3	11.4
10	3.6	2.6	3.9	6.8

negligible contribution, since their values (depending on the port) range between -1.2 cm and -2.0 cm for scenario RCP4.5 – 2045, -0.3 cm and -1.1 cm for scenario RCP8.5 – 2045, -0.7 cm to -1.4 cm for scenario RCP4-5 – 2100 and -3,8 cm to -4.4 cm for scenario RCP8.5 – 2100.

Therefore, the worst case, as it could be expected, is scenario RCP8.5 in 2100, in which 90.4% of docks and 67.9% of piers become inoperative. In addition, in this scenario, 26 ports (78.8%) have all their dock length inoperative and 15 ports (45.5%) have all the piers inoperative due to the large SLR (88 cm) projected. In the same year, but considering scenario RCP4.5, the smaller SLR (47 cm) leads to a shorter affected length (64.6% for ports and 41.4% of piers) and to a significantly lower number of ports with their berthing structures totally inoperative: 8 (24.2%) for docks and 6 (18.2%) for piers. This highlights how SLR values condition the results for inoperability of berthing structures. On the contrary, in 2045, there are far fewer inoperative berthing structures: around 10% under scenario RCP4.5 and around 20% under scenario RCP8.5 of their total length.

It must be noticed that there are 6 ports (18.2%) with no piers affected by SLR. In 4 of them, this is because they do not have such type of berthing structure and in the other 2 because all the piers are floating ones.

Analyzing data from Tables 3 and 4 an increase of the amount of inoperative structures and adaptation costs can be observed, directly related with SLR. Nevertheless, such increases do not vary linearly with SLR. For example, in scenario RCP8.5 – 2045, the value of SLR is 1.4 times that of scenario RCP4.5 – 2045, while the length ratio of inoperative structures and adaptation costs are 2 and 2.1 respectively. In 2100 scenarios, this magnification effect is greatly enlarged and under scenario RCP4.5 - 2100 the ratios with respect the values for scenario RCP4.5 – 2045 are 2.6 for SLR, 5.5 for inoperative structure length and 7.2 for adaptation costs, while under scenario RCP8.5 - 2100 these ratios are 4.9 (SLR), 7.9 (length of inoperative structures) and 15.8 (costs). Therefore, for horizon 2100, the impacts of SLR on inoperability of berthing structures due to insufficient freeboard will be very large, as well as the adaptation costs. Indeed, this impact will be the worst that the studied ports will have to face during the 21st century due to climate change.

6 Concluding remarks

In this work, the impacts of climate change on berthing structures in the ports of Balearic Islands have been assessed. These impacts have been quantified in terms of port agitation and inoperability of berthing structures due to insufficient freeboard, for two climate scenarios (RCP4.5 and RCP8.5) and two time horizons (2045 and 2100). This study is the first that analyses the impact of climate change on port berthing structures at regional scale with this level of detail and considering all the driving factors: sea-level rise, waves, tide and storm surge.

The results show that the port inoperability due to an excess of wave agitation will not change significantly during the 21st century because wave conditions will be barely modified and even future wave heights will be slightly smaller than at the present situation. In this case, the variations in agitation will be due to changes in wave propagation patterns induced by SLR. The adaptation costs to such impact will be of the order of 30 million euros (in current monetary units).

On the contrary, the most significant impact on the studied ports will be the reduction of operability of berthing structures due to insufficient freeboard as a result of SLR. Although in 2045 such impact will be smaller with 10.5% of structures affected under scenario RCP4.5 or 20.5% under scenario RCP8.5, in 2100 57.1% (RCP4.5) or 83.2% (RCP8.5) of such structures will be inoperative. Although this impact is directly related to SLR, the relationship between them is non-linear and there is a magnification effect of such impact when sea-level rises. In the same way, the adaptation costs greatly increase with SLR and they are estimated in 6.45 M€ (RCP4.5 – 2045), 13.33 M€ (RCP8.5 – 2045), 46.53 M€ (RCP4.5 – 2100) and 101.86 M€ (RCP8.5 – 2100) in current monetary units. This illustrates the magnitude of the impact of SLR on port operability, in particular by the end of the century.

Data availability statement

The raw data supporting the conclusions of this article will be made available by the authors, without undue reservation.

Author contributions

JPS, AS-A, MB, and CB designed the research. CM, DG-M, and JG collected, prepared and analyzed the data. JPS, XG, VG, and CA carried out the numerical simulations. JPS and AS-A wrote the manuscript, with contributions from other authors. All authors contributed to the article and approved the submitted version.

Funding

This study was supported by PIMA ADAPTA-Balears Project funded by Conselleria de Transició Energética, Sectors Productius i Memòria Democràtica and Conselleria de Mobilitat i Habitatge, Govern Balear, and by the project PLEC2021-007810 funded by MCIN/AEI/10.13039/501100011033 and by the European Union "Next Generation EU"/PRTR".

Acknowledgments

The authors wish to acknowledge Puertos del Estado and Instituto de Hidráulica Ambiental de la Universidad de Cantabria (IHC) for providing the data used in the study. The support of the Departament de Recerca i Universitats de la Generalitat de Catalunya (Ref. 2021SGR00600) is also acknowledged.

Conflict of interest

The authors declare that the research was conducted in the absence of any commercial or financial relationships that could be construed as a potential conflict of interest.

Publisher's note

References

Agulles, M., Jordà, G., and Lionello, P. (2021). Flooding of sandy beaches in a changing climate. The case of the Balearic Islands (NW Mediterranean). *Front. Mar. Sci.* 8. doi: 10.3389/fmars.2021.760725

Alvarez-Ellacuria, A., Orfila, A., Gómez-Pujol, L., Simarro, G., and Obregon, N. (2011). Decoupling spatial and temporal patterns in short-term beach shoreline response to wave climate. *Geomorphology* 128, 199–208. doi: 10.1016/j.geomorph.2011.01.008

Amarouche, K., Bingölbali, B., and Akpinar, A. (2022). New wind-wave climate records in the Western Mediterranean Sea. *Clim. Dyn.* 58, 1899–1922. doi: 10.1007/s00382-021-05997-1

Becker, A., Inoue, S., Fischer, M., and Schwegler, B. (2012). Climate change impacts on international seaports: knowledge, perceptions, and planning, efforts among port administrations. *Clim. Change* 110, 5–29. doi: 10.1007/s10584-011-0043-7

Belloti, G. (2007). Transient response of harbours to long waves under resonance conditions. *Coast. Eng.* 54, 680–693. doi: 10.1016/j.coastaleng.2007.02.002

Belloti, G., and Franco, L. (2011). Measurement of long waves at the harbor of Marina de Carrara, Italy. *Ocean Dyn.* 61, 2051–2059. doi: 10.1007/s10236-011-0468-6

Bevacqua, E., Maraun, D., Vousdoukas, M. I., Voukouvalas, E., Vrac, M., Mentaschi, L., et al. (2019). Higher probability of compound flooding from precipitation and storm surge in Europe under anthropogenic climate change. *Adv. Sci.* 5, eaaw5531. doi: 10.1016/j.apgeog.2018.07.023

Bonaduce, A., Pinardi, N., Oddo, P., Spada, G., and Larnicol, G. (2016). Sea-level variability in the Mediterranean Sea from altimetry and tide gauges. *Clim. Dyn.* 47, 2851–2866. doi: 10.1007/s00382-016-3001-2

Bonaldo, D., Bucchignani, E., Pomaro, A., Ricchi, A., Sclavo, M., and Carniel, S. (2020). Wind waves in the Adriatic Sea under a severe climate change scenario and implications for the coasts. *Int. J. Climatol.* 40, 5389–5406. doi: 10.1002/joc.6524

Bon de Sousa, L., Loureiro, C., and Ferreira, O. (2018). Morphological and economic impacts of rising sea levels on cliff-backed platform beaches in southern Portugal. *Appl. Geogr.* 99, 31–43. doi: 10.1016/j.apgeog.2018.07.023

Booij, N., Ris, R. C., and Holthuijsen, L. H. (1999). A third-generation wave model for coastal regions: 1. Model description and validation. *J. Geophys. Res.* 104, 7649–7666.

Brown, S., and Nicholls, R. J. (2015). Subsidence and human influences in mega deltas: the case of the Ganges–Brahmaputra–Meghna. *Sci. Total Environ.* 527–528, 362–374. doi: 10.1016/j.scitotenv.2015.04.124

Brown, S., Nicholls, R. J., Lowe, J. A., and Hinkel, J. (2013). Spatial variations of sea-level rise and impacts: an application of DIVA. *Clim. Change*. 134, 403–416. doi: 10.1007/s10584-013-0925-y

Campins, J., Genovés, A., Picornell, M. A., and Jansà, A. (2011). Climatology of Mediterranean cyclones using the ERA-40 dataset. *Int. J. Climatol.* 31, 1596–1614. doi: 10.1002/joc.2183

Campos, A., García-Valdecasas, J. M., Molina, R., Castillo, C., Álvarez-Fanjul, E., and Staneva, J. (2019). Addressing long-term operational risk management in port docks under climate change scenarios. *Water* 11, 2153. doi: 10.3390/w11102153

Camus, P., Tomás, A., Díaz-Hernández, G., Rodríguez, B., Izaguirre, C., and Losada, I. J. (2019). Probabilistic assessment of port operation downtimes under climate change. *Coast. Eng.* 147, 12–24. doi: 10.1016/j.coastaleng.2019.01.007

Casas-Prat, M., and Sierra, J. P. (2010). Trend analysis of wave storminess: wave direction and its impact on harbour agitation. *Nat. Hazard Earth Syst. Sci.* 10, 2327–2340. doi: 10.5194/nhess-10-2327-2010

Casas-Prat, M., and Sierra, J. P. (2012). Trend analysis of wave direction and associated impacts on the Catalan coast. *Clim. Change* 115, 667–691. doi: 10.1007/s10584-012-0466-9

Casas-Prat, M., and Sierra, J. P. (2013). Projected future wave climate in the NW Mediterranean Sea. *J. Geophys. Res. Oceans* 118, 3548–3568. doi: 10.1002/jgrc.20233

Casas-Prat, M., Wang, X. L., and Swart, N. (2018). CMIP5-based global wave climate projections including the entire Arctic Ocean. *Ocean Model.* 123, 66–85. doi: 10.1016/j.ocemod.2017.12.003

Cavaleri, L., Bertotti, L., Torrisi, L., Bitner-Gregersen, E., Serio, M., and Onorato, M. (2012). Rogue waves in crossing seas: the Louis Majesty accident. *J. Geophys. Res.* 117, C00J10. doi: 10.1029/2012JC007923

Chhetri, P., Cocoran, J., Gekara, V., Maddox, C., and McEvoy, D. (2015). Seaport resilience to climate change: mapping vulnerability to sea-level rise. *J. Spat. Sci.* 60, 65–78. doi: 10.1080/14498596.2014.943311

Chhetri, P., Jayatilleke, G. B., Gekara, V. O., Manzoni, A., and Corbitt, B. (2016). Container terminal operations simulator (CTOS)–Simulating the impact of extreme weather events on port operation. *Europ. J. Transp. Infrast.* 16, 195–213. doi: 10.18757/ejtir.2016.16.1.3121

Conte, D., and Lionello, P. (2013). Characteristics of large positive and negative surges in the Mediterranean Sea and their attenuation in future climate scenarios. *Glob. Planet. Change* 111, 159–173. doi: 10.1016/j.gloplacha.2013.09.006

Conte, D., and Lionello, P. (2014). Storm surge distribution along the Mediterranean coast: Characteristics and evolution. *Procedia. Soc. Behav. Sci.* 120, 110–115. doi: 10.1016/j.sbspro.2014.02.087

Contestabile, P., Crispino, G., Russo, S., Gisonni, C., Cascetta, F., and Vicinanza, D. (2020). Crown wall modifications as response to wave overtopping under a future sea level scenario: An experimental parametric study for an innovative composite seawall. *Appl. Sci.* 10, 2227. doi: 10.3390/app10072227

Cousineau, J., and Murphy, E. (2022). Numerical investigation of climate change effects on storm surges and extreme waves on Canada's Pacific coast. *Atmosphere* 13, 311. doi: 10.3390/atmos13020311

Dangendorf, S., Marcos, M., Wöppelmann, G., Conrad, C. P., Frederikse, T., and Riva, R. (2017). Reassessment of 20th century global mean sea level rise. *Proc. Natl. Acad. Sci. U. S. A.* 114, 5946–5951. doi: 10.1073/pnas.1616007114

de Alfonso, M., Lin-Ye, J., García-Valdecasas, J. M., Pérez-Rubio, S., Luna, M. Y., Santos-Muñoz, D., et al. (2021). Storm Gloria: sea state evolution based on *in situ* measurements and modeled data and its impact on extreme values. *Front. Mar. Sci.* 8. doi: 10.3389/fmars.2021.646873

Dee, D. P., Uppala, S. M., Simmons, A. J., Berrisford, P., Poli, P., Kobayashi, S., et al. (2011). The ERA-Interim reanalysis: configuration and performance of the dataassimilation system. *Q. J. R. Meteorol. Soc* 137. doi: 10.3389/fmars.2021.709595

de Leo, F., Besio, G., Briganti, R., and Vanem, E. (2021a). Non-stationary extreme value analysis of sea states based on linear trends. Analysis of annual maxima series of significant wave height and peak period in the Mediterranean Sea. *Coast. Eng.* 167, 103896. doi: 10.1016/j.coastaleng.2021.103896

de Leo, F., Besio, G., and Mentaschi, L. (2021b). Trends and variability of ocean waves under RCP8.5 emission scenario in the Mediterranean Sea. *Ocean Dyn.* 71, 97–117. doi: 10.1007/s10236-020-01419-8

Durand, G., van den Broeke, M. R., Le Cozannet, G., Edwards, T. L., Holland, P. R., Jourdain, N. C., et al. (2022). Sea-level rise: from global to local perspectives. *Front. Mar. Sci.* 8, 709595. doi: 10.3389/fmars.2021.709595

Echevarria, E. R., Hemer, M. A., and Holbrook, N. J. (2019). Seasonal variability of the global spectral wind wave climate. *J. Geophys. Res.* 124, 2924–2939. doi: 10.5194/nhess-17-1075-2017

Enríquez, A. R., Marcos, M., Álvarez-Ellacuría, A., Orfila, A., and Gomis, D.. (2017). Changes in beach shoreline due to sea level rise and waves under climate change scenarios: application to the Balearic Islands (western Mediterranean). *Nat. Hazards Earth Syst.* 17, 1075–1089. doi: 10.5194/nhess-17-1075-2017

Enríquez, A. R., Marcos, M., Falqués, A., and Roelvink, D. (2019). Assessing beach and dune erosion and vulnerability under sea level rise: A case study in the Mediterranean Sea. *Front. Mar. Sci.* 6. doi: 10.3389/fmars.2019.00004

EPPE (2000). "ROM ROM 3.1-99," in *Design of the maritime configuration of ports, approach channels and harbour basins. Recommendations for maritime works* (Madrid: Puertos del Estado, Ministerio de Fomento), 327.

EPPE (2012). "ROM 0.2-11," in *Recomendaciones para el proyecto y ejecución de obras de atraque y amarre* (Madrid, Spain: Puertos del Estado, Ministerio de Fomento), 465.

EPPE (2019). *REDMAR: Red de mareógrafos de Puertos del Estado.Puerto de Palma* (Madrid, Spain: Puertos del Estado, Ministerio de Fomento), 31.

EPPE (2021). *Extremos máximos de oleaje por direcciones (altura de ola significante). Boya de Dragonera. Banco de datos oceanográficos de Puertos del Estado* (Madrid, Spain: Puertos del Estado, Ministerio de Fomento), 14.

Ferrante, M., Conti, G. O., Fiore, M., Rapisarda, V., and Ledda, C. (2013). Harmful algal blooms in the mediterranean sea: effects on human health. *EuroMediterranean Biomed. J.* 8, 25–34. doi: 10.3269/1970-5492.2013.8.6

Giorgi, F. (2006). Climate change hot-spots. *Geophys. Res. Lett.* 33, L08707. doi: 10.1029/2006GL025734

Goharnejad, H., Perrie, W., Toulany, B., Casey, M., and Zhang, M. (2022). Clustering of climate chamge impacts on ocean waves in the Northwest Atlantic. *J. Atmos. Ocean Tech.* 39, 237–257. doi: 10.1175/JTECH-D-21-0053.1

González-Marco, D., Sierra, J. P., Fernández de Ybarra, O., and Sánchez-Arcilla, A. (2008). Implications of long waves in harbour management: The Gijon port case study. *Ocean Coast. Manage.* 51, 180–201. doi: 10.1016/j.ocecoaman.2007.04.001

Gracia, V., Sierra, J. P., Gomez, M., Pedrol, M., Sampé, S., García-León, M., et al. (2019). Assessing the impact of sea level rise on operability using LIDAR-derived digital elevation models. *Remote Sens. Environ.* 232, 111318. doi: 10.1016/j.rse.2019.111318

Grases, A., Gracia, V., García-León, M., Lin-Ye, J., and Sierra, J. P. (2020). Coastal flooding and erosion under a changing climate: implications at a low-lying coast (Ebro Delta). *Water* 12, 346. doi: 10.3390/w12020346

Gregory, J. M., White, N. J., Church, J. A., Bierkens, M. F. P., Box, J. E., van der Broeke, M. R., et al. (2013). Twentieth-century global-mean sea level rise: is the whole greater than the sum of the parts? *J. Clim.* 26, 4476–4499. doi: 10.1175/JCLI-D-12-00319.1

Hanson, S. E., and Nicholls, R. J. (2020). Demand for ports to 2050: Climate policy, growing trade and the impacts of sea-level rise. *Earth's Future* 8, e2020EF001543. doi: 10.1029/2020EF001543

Hanson, S., Nicholls, R., Ranger, N., Hallegate, S., Corfee-Morlot, J., Herweijer, C., et al. (2011). A global ranking of port cities with high exposure to climate extremes. *Clim. Change* 104, 89–111. doi: 10.1007/s10584-010-9977-4

Hemer, M. A., Fan, Y., Mori, N., Semedo, A., and Wang, X. L. (2013b). Projected change in wave climate from a multi-model ensemble. *Nat. Clim. Change* 3, 471–476. doi: 10.1038/nclimate1791

Hemer, M. A., Katzfey, J., and Trenham, C. E. (2013a). Global dynamical projections of surface ocean wave climate for a future high greenhouse gas emission scenario. *Ocean Model.* 70, 221–245. doi: 10.1016/j.ocemod.2012.09.008

Hemer, M. A., and Trenham, C. E. (2016). Evaluation of a CMIP5 derived dynamical global wind wave climate model ensemble. *Ocean Model.* 103, 190–223. doi: 10.1016/j.ocemod.2015.10.009

Hilmi, N., Allemand, D., Cinar, M., Cooley, S., Hall-Spencer, J. M., Haraldsson, G., et al. (2014). Exposure of mediterranean countries to ocean acidification. *Water* 6, 1719–1744. doi: 10.3390/w6061

Hinkel, J., Jaeger, C., Nicholls, R. J., Lowe, J., Renn, O., and Peijun, S. (2015). Sea-level risk scenarios and coastal risk management. *Nat. Clim. Change* 5, 188–190. doi: 10.1038/nclimate2505

Hsiao, S.-C., Chiang, W.-S., Jang, J.-H., Wu, H.-L., Lu, W.-S., Chen, W.-B., et al. (2021). Flood risk influenced by the compound effect of storm surge and rainfall under climate change for low-lying coastal areas. *Sci. Total Environ.* 764, 144439. doi: 10.1016/j.scitotenv.2020.144439

IPCC (2013). "Climate change 2013. The physical science basis," in *Contribution of working Group I to the fifth assessment report of the intergovernmental panel on climate change*. Eds. T. F. Stocker, D. Qin, G.-K. Plattner, M. Tignor, S. K. Allen, J. Boschung, et al (Cambridge, United Kingdom and New York, NY, USA: Cambridge University Press), 1535.

IPCC (2021). "Climate change 2021: the physical science basis," in *Contribution of working Group I to the sixth assessment report of the intergovernmental panel on climate change*. Eds. V. Masson-Delmotte, P. Zhai, A. Pirani, S. L. Connors, C. Péan, S. Berger, et al (United Kingdom and New York, NY, USA: Cambridge University Press, Cambridge), 2391.

Izaguirre, C., Losada, I. J., Camus, P., Vigh, J. L., and Stenek, V. (2021). Climate change risk to global port operations. *Nat. Clim. Change* 11, 14–20. doi: 10.1038/s41558-020-00937-z

Jebbad, R., Sierra, J. P., Mösso, C., Mestres, M., and Sánchez-Arcilla, A. (2022). Assessment of harbour inoperability and adaptation cost due to sea level rise. Application to the port of Tangier-Med (Morocco). *Appl. Geogr.* 138, 102623. doi: 10.1016/j.apgeog.2021.102623

Jevrejeva, S., Grinsted, A., and Moore, J. C. (2014). Upper limit for sea level projections by 2100. *Environ. Res. Lett.* 9, 104008. doi: 10.1088/1748-9326/9/10/104008

Jevrejeva, S., Moore, J. C., and Grinsted, A. (2012). Sea level projections to AD2500 with a new generation of climate change scenarios. *Glob. Planet. Change* 80–81, 14–20. doi: 10.1016/j.gloplacha.2011.09.006

Jordà, G., Gomis, D., Álvarez-Fanjul, E., and Somot, S. (2012). Atmospheric contribution to Mediterranean and nearby Atlantic Sea level variability under different climate change scenarios. *Glob. Planet. Change* 80, 198–214. doi: 10.1016/j.gloplacha.2011.10.013

Juza, M., and Tintoré, J. (2021). Mutivariate sub-regional ocean indicators in the Mediterranean Sea: From event detection to climate change estimations. *Front. Mar. Sci.* 8. doi: 10.3389/fmars.2021.610589

Kapelonis, Z. G., Graviliadis, P. N., and Athanassoulis, A. (2015). Extreme value analysis of dynamical wave climate projections in the Mediterranean Sea. *Proc. Comput. Sci.* 66, 210–219. doi: 10.1016/j.procs.2015.11.025

Kassis, D., and Varlas, G. (2021). Hydrographic effects of an intense "medicane" over the central-eastern Mediterranean Sea in 2018. *Dyn. Atmos. Oceans* 93, 101185. doi: 10.1016/j.dynatmoce.2020.101185

Kotlarski, S., Keuler, K., Christensen, O. B., Colette, A., Déqué, M., Gobiet, A., et al. (2014). Regional climate modeling on European scales: a joint standard evaluation of the EURO-CORDEX RCM ensemble. *Geosci. Model. Dev.* 7, 1297–1333. doi: 10.5194/gmd-7-1297-2014

Lacoue-Labarthe, T., Nunes, P. A. L. D., Ziveri, P., Cinar, M., Gazeau, F., Hall-Spencer, J. M., et al. (2016). Impacts of ocean acidification in a warming Mediterranean Sea: an overview. *Region. Stud. Mar. Sci.* 5, 1–11. doi: 10.1016/j.rsma.2015.12.005

Leal, K. B., Robaina, L. E. S., and De Lima, A. S. (2022). Coastal impacts of storm surge on a changing climate: a global bibliometric analysis. *Nat. Hazards* 114, 1455–1476. doi: 10.1007/s11069-022-05432-6

Lesani, S., and Niksokhan, M. H. (2019). Climate change impact on Caspian Sea wave conditions in the Noshahr port. *Ocean Dyn.* 69, 1287–1310. doi: 10.1007/s10236-019-01313-y

Li, M., Zhang, F., Barnes, S., and Wang, X. (2020). Assessing storm surge impacts on coastal inundation due to climate change: case studies of Baltimore and Dorchester County in Maryland. *Nat. Hazards* 103, 2561–2588. doi: 10.1007/s11069-020-04096-4

Lin-Ye, J., García-León, M., Gràcia, V., Ortego, M. I., Lionello, P., Conte, D., et al. (2020). Modeling of future extreme storm surges at the NW Mediterranean Coast (Spain). *Water* 12, 472. doi: 10.3390/w12020472

Lionello, P., Cogo, S., Galati, M. B., and Sanna, A. (2008). The Mediterranean surface wave climate inferred from future scenario simulations. *Glob. Planet. Change* 63, 152–162. doi: 10.1016/j.gloplacha.2008.03.004

Lionello, P., Conte, D., Marzo, L., and Scarascia, L. (2017). The contrasting effect of increasing mean sea level and decreasing storminess on the maximum level during

storms along the coast of the Mediterranean Sea in the mid 21st century. *Glob. Planet. Change* 151, 80–91. doi: 10.1016/j.gloplacha.2016.06.012

Lionello, P., and Giorgi, F. (2007). Winter precipitation and cyclones in the Mediterranean Region: Future climate scenarios in a regional simulation. *Adv. Geosci.* 12, 153–158. Available at: www.adv-geosci.net/12/153/2007/.

Lionello, P., Mufato, R., and Tomasin, A. (2005). Sensitivity of free and forced oscillations of the Adriatic Sea to sea level rise. *Clim. Res.* 29, 23–39.

Lionello, P., and Sanna, A. (2005). Mediterranean wave climate variability and its links with NAO and Indian monsoon. *Clim. Dyn.* 26, 611–623. doi: 10.1007/s00382-005-0025-4

Lionello, P., and Scarascia, L. (2018). The relation between climate change in the Mediterranean region and global warming. *Reg. Environ. Change* 18, 1481–1493. doi: 10.1007/s10113-018-1290-1

Lira-Loarca, A., and Besio, G. (2022). Future changes and seasonal variability of the directional wave spectra in the Mediterranean Sea for the 21st century. *Environ. Res. Lett.* 17, 104015. doi: 10.1088/1748-9326/ac8ec4

Lira-Loarca, A., Cobos, M., Besio, G., and Baquerizo, A. (2021). Projected wave climate temporal variability due to climate change. *Stoch. Env. Res. Risk A.* 35, 1741–1757z. doi: 10.1007/s00477-020-01946-2

Lobeto, H., Menendez, M., and Losada., I. J. (2021a). Future behaviour of wind wave extremes due to climate change. *Sci. Rep.* 11, 7869. doi: 10.1038/s41598-021-86524-4

Lobeto, H., Menendez, M., and Losada., I. J. (2021b). Projections of directional spectra help to unravel the future behavior of wind waves. *Front. Mar. Sci.* 8. doi: 10.3389/fmars.2021.655490

López, I., López, M., and Iglesias, G. (2015). Artificial neural networks applied to port operability assessment. *Ocean Eng.* 109, 298–308. doi: 10.1016/j.oceaneng.2015.09.016

Lorente, P., Lin-Ye, J., García-León, M., Reyes, E., Fernandes, M., Sotillo, M. G., et al. (2021). On the performance of high frequency radar in the Western Mediterranean during the record-breaking storm Gloria (2021). *Front. Mar. Sci.* 8. doi: 10.3389/fmars.2021.645762

Loza, P., and Veloso-Gomes, F. (2023). Literature review on incorporating climate change adaptation measures in the design of new ports and other maritime projects. *Sustainability* 15, 4569. doi: 10.3390/su15054569

Luque, P., Gómez-Pujol, L., Marcos, M., and Orfila, A. (2021). Coastal flooding in the Balearic Islands during the twenty-first century caused by sea-level rise and extreme events. *Front. Mar. Sci.* 8. doi: 10.3389/fmars.2021.676452

Malej, M., Shi, F., Smith, J. M., Cuomo, G., and Tozer, N. (2021). Boussinesq-type modelling of low-frequency wave motions at Marina di Carrara. *J. Waterway Port Coastal Ocean Eng.* 147, 05021015. doi: 10.1061/(ASCE)WW.1943-5460.0000676

Maravelakis, N., Kalligeris, N., Lynett, P. J., Skanavis, V. L., and Synolakis, C. E. (2021). Wave overtopping due to harbour resonance. *Coast. Eng.* 169, 103973. doi: 10.1016/j.coastaleng.2021.103973

Marcos, M., Jordà, G., Gomis, D., and Pérez, B. (2011). Changes in storm surges in southern Europe from a regional model under climate change scenarios. *Glob. Planet. Change* 77, 116–128. doi: 10.1016/j.gloplacha.2011.04.002

Marcos, M., Tsimplis, M. N., and Shaw, A. G. P. (2009). Sea level extremes in southern Europe. *J. Geophys. Res.* 114, C01007. doi: 10.1029/2008JC004912

Mase, H., Tsujio, D., Yasuda, T., and Mori, N. (2013). Stability analysis of composite breakwater with wave-dissipating blocks considering increase in sea levels, surges and waves due to climate change. *Ocean Eng.* 71, 58–65. doi: 10.1016/j.oceaneng.2012.12.037

Meucci, A., Young, I. R., Hemer, M., Kirezci, E., and Ranasinghe, R. (2020). Projected 21st century changes in extreme wind-wave events. *Sci. Adv.* 6, 7295–7305. doi: 10.1126/sciadv.aaz7295

Milglietta, M. M., and Rotunno, R. (2019). Development mechanisms for Mediterranean tropical-like cyclones (medicanes). *Q. J. R. Meteorol. Soc* 145, 1444–1460. doi: 10.1002/qj.3503

Mitchell, J. F., Lowe, J., Wood, R. A., and Vellinga, M. (2006). Extreme events due to human-induced climate change. *Philos. Trans. R. Soc A Math. Phys. Eng. Sci.* 364, 2117–2133. doi: 10.1098/rsta.2006.1816

Morales-Márquez, V., Orfila, A., Simarro, G., and Marcos, M. (2020). Extreme waves and climatic patterns of variability in the eastern North Atlantic and Mediterranean basins. *Ocean Sci.* 16, 1385–1398. doi: 10.5194/os-16-1385-2020

Mori, N., Shimura, T., Yasuda, T., and Mase, H. (2013). Multi-model climate projections of ocean surface variables under different climate scenarios: future change of waves, sea level and wind. *Ocean Eng.* 71, 122–129. doi: 10.1016/j.oceaneng.2013.02.016

Morim, J., Hemer, M., Cartwright, N., Strauss, D., and Andutta, F. (2018). On the concordance of 21st century wind-wave climate projections. *Glob. Planet. Change* 167, 160–171. doi: 10.1016/j.gloplacha.2018.05.005

Morim, J., Vitousek, S., Hemer, M., Reguero, B., Erikson, L., Casas-Prat, M., et al. (2021). Global scale changes to extreme ocean wave events due to anthropogenic warming. *Environ. Res. Lett.* 16, 074056. doi: 10.1088/1748-9326/ac1013

Ng, A. K. Y., Chen, S., Cahoon, S., Brooks, B., and Yang, Z. (2013). Climate change and the adaptation strategies of ports: The Australian experiences. *Res. Transport. Bus. Manage.* 8, 186–194. doi: 10.1016/j.rtbm.2013.05.005

Ng, A. K. Y., Zhang, H., Afenyo, M., Becker, A., Cahoon, S., Chen, S., et al. (2018). Port decision maker perceptions on the effectiveness of climate adaptation actions. *Coast. Manage.* 46 (3), 148–175. doi: 10.1080/08920753.2018.1451731

Nicholls, R. J., and Cazenave, A. (2010). Sea-level rise and its impacts on coastal zones. *Science* 328, 1517–1520. doi: 10.1126/science.1185782

Nicholls, R. J., Marinova, N., Lowe, J. A., Brown, S., Gusmão, D., Hinkel, J., et al. (2011). Sea-level rise and its possible impacts given a 'beyond 4 °C world' in the twenty-first century. *Philos. Trans. R. Soc A Math. Phys. Eng. Sci.* 369, 161–181. doi: 10.1098/rsta.2010.0291

Nicholls, R. J., Wong, P. P., Burkett, V., Woodroffe, C. D., and Hay, J. (2008). Climate change and coastal vulnerability assessment: scenarios for integrated assessment. *Sustain. Sci.* 3, 89–102. doi: 10.1007/s11625-008-0050-4

Nursey-Bray, M., Blackwell, B., Brooks, B., Campbell, M. L., Goldsworthy, L., Pateman, H., et al. (2013). Vulnerabilities and adaptation of ports to climate change. *J. Environ. Plan. Manage.* 56, 1021–1045. doi: 10.1080/09640568.2012.716363

Orejarena-Rondón, A. F., Sayol, J. M., Marcos, M., Otero, L., Restrepo, J. C., Hernández-Carrasco, I., et al. (2019). Coastal impacts driven by sea-level rise in Cartagena de Indias. *Front. Mar. Sci.* 6. doi: 10.3389/fmars.2019.00614

Orfila, A., Jordi, A., Basterretxea, G., Vizoso, G., Marbà, N., Duarte, C., et al. (2005). Residence time and Posidonia oceanica in Cabrera Archipelago National Park, Spain. *Cont. Shelf Res.* 25, 1339–1352. doi: 10.1016/j.csr.2005.01.004

Pillai, K., Lemckert, C., Etemad-Shahidi, A., Cappieti, L., and Sigurdarson, S. (2019). Effect of sea level rise on wave overtopping rate at berm breakwater. *J. Waterway Port Coastal Ocean Eng.* 145, 04019019. doi: 10.1061/(ASCE)WW.1943-5460.0000522

Portilla-Yandun, J., Salazar, A., and Cavaleri, L. (2016). Climate patterns derived from ocean wave spectra. *Geophys. Res. Lett.* 43, 11736–11743. doi: 10.1002/2016GL071419

Portillo Juan, N., Negro Valdecantos, V., and del Campo, J. M. (2022). Review of the impacts of climate change on ports and harbours and their adaptation in Spain. *Sustainability* 14, 7507. doi: 10.3390/su14127507

Pritchard, H. D., and Vaughan, D. G. (2007). Widespread acceleration of tidewater glaciers on the antarctic peninsula. *J. Geophys. Res.* 112, F03S29. doi: 10.1029/2006JF000597

Rahmstorf, S. (2007). Sea-level rise a semi-empirical approach to projecting future. *Science* 315, 368–370. doi: 10.1126/science.1135456

Rahmstorf, S. (2017). Rising hazard of storm surge flooding. *P. Nat. Acad. Sci. U.S.A.* 114, 11806–11808. doi: 10.1073/pnas.1715895114

Ramírez, M., Menéndez, M., Camus, P., and Losada, I. J. (2019). *Elaboración de la metodología y bases de datos para la proyección de impactos de cambio climático a lo largo de la costa española. Tarea 2: Proyecciones de alta resolución de variables marinas en la costa española* (Santander, Spain: Instituto de Hidráulica Ambiental, Universidad de Cantabria), 63.

Ranasinghe, R. (2016). Assessing climate change impacts on open sandy coasts: a review. *Earth-Sci. Rev.* 160, 320–332. doi: 10.1016/j.earscirev.2016.07.011

Revell, D. L., Battalio, R., Spear, B., Ruggiero, P., and Vandever, J. (2011). A methodology for predicting future coastal hazards due to sea-level rise on the California coast. *Clim. Change* 1091, S251–S276. doi: 10.1007/s10584-011-0315-2

Ris, R. C., Holthuijsen, L. H., and Booij, N. (1999). A third-generation wave model for coastal regions: 2. Verification. *J. Geophys. Res.* 104, 7667–7681.

Rusu, L., and Guedes Soares, C. (2013). Evaluation of a high-resolution wave forecasting system for the approaches to ports. *Ocean Eng.* 58, 224–238. doi: 10.1016/j.oceaneng.2012.11.008

Ruti, P. M., Somot, S., Giorgi, F., Dubois, C., Flaounas, E., Obermann, A., et al. (2016). Med-CORDEX initiative for Mediterranean climate studies. *B. Am. Meteorol. Soc* 97, 1187–1208. doi: 10.1175/BAMS-D-14-00176.1

Ryabinin, V., Barbière, J., Haugan, P., Kullenberg, G., Smith, N., McLean, C., et al. (2019). The UN Decade of ocean science for sustainable development. *Front. Mar. Sci.* 6. doi: 10.3389/fmars.2019.00470

Sánchez-Arcilla, A., González-Marco, D., and Bolaños, R. (2008). A review of wave climate and prediction along the Spanish Mediterranean coast. *Nat. Hazards Earth Syst. Sci.* 8, 1217–1228. doi: 10.5194/nhess-8-1217-2008

Sánchez-Arcilla, A., Mösso, C., Sierra, J. P., Mestres, M., Harzallah, A., Senouci, M., et al. (2011). Climate drivers of potential hazards in Mediterranean coasts. *Reg. Environ. Change* 11, 617–636. doi: 10.1007/s10113-010-0193-6

Sánchez-Arcilla, A., Sierra, J. P., Brown, S., Casas-Prat, M., Nicholls, R. J., Lionello, P., et al. (2016). A review of potential physical impacts on harbours in the Mediterranean Sea under climate change. *Reg. Environ. Change* 16, 2471–2484. doi: 10.1007/s10113-016-0972-9

Sayol, J. M., and Marcos, M. (2018). Assessing flood risk under sea level rise and extreme sea levels scenarios: application to the Ebro Delta (Spain). *J. Geophys. Res. Oceans* 123, 794–811. doi: 10.1002/2017JC013355

Scarascia, L., and Lionello, P. (2013). Global and regional factors contributing to the past and future sea level rise in the Northern Adriatic Sea. *Glob. Planet. Change* 106, 51–63. doi: 10.1016/j.gloplacha.2013.03.004

Shchepetkin, A. F., and McWilliams, J. C. (2005). The regional oceanic modelling system (ROMS): a split-explicit, free-surface, topography-following coordinate oceanic model. *Ocean Model.* 9, 347–404. doi: 10.1016/j.ocemod.2004.08.002

Shimura, T., and Mori, N. (2019). High-resolution wave climate hindcast around Japan and its spectral representation. *Coast. Eng.* 151, 1–9. doi: 10.1016/j.coastaleng.2019.04.013

Sierra, J. P. (2019). Economic impact of overtopping and adaptation measures in Catalan ports due to sea level rise. *Water* 11, 1440. doi: 10.3390/w11071440

Sierra, J. P., Casanovas, I., Mösso, C., Mestres, M., and Sánchez-Arcilla, A. (2016). Vulnerability of Catalan (NW Mediterranean) ports to wave overtopping due to different scenarios of sea level rise. *Reg. Environ. Change* 16, 1457–1468. doi: 10.1007/s10113-015-0879-x

Sierra, J. P., and Casas-Prat, M. (2014). Analysis of potential impacts on coastal areas due to changes in wave conditions. *Clim. Change* 124, 861–876. doi: 10.1007/s10584-014-1120-5

Sierra, J. P., Casas-Prat, M., Virgili, M., Mösso, C., and Sánchez-Arcilla, A. (2015). Impacts on wave-driven harbour agitation due to climate change in Catalan ports. *Nat. Hazard Earth Syst. Sci.* 15, 1695–1709. doi: 10.5194/nhess-15-1695-2015

Sierra, J. P., Genius, A., Lionello, P., Mestres, M., Mösso, C., and Marzo, L. (2017). Modelling the impact of climate change on harbour operability: the Barcelona port case study. *Ocean Eng.* 141, 64–78. doi: 10.1016/j.oceaneng.2017.06.002

Sierra, J. P., Sánchez-Arcilla, A., Egozcue, J. J., and Monsó, J. L. (1988). "Effect of Boussinesq-type equations on wave spectra propagation," in *Proceedings, 21st International Conference on Coastal Engineering.* (Malaga, Spain: American Society of Civil Engineers) 350–362.

Slangen, A. B. A., Carson, M., Katsman, C. A., van de Wal, R. S. W., Köhl, A., Vermeersen, L. L. A., et al. (2014). Projecting twenty-first century regional sea-level changes. *Clim. Change* 124, 327–332. doi: 10.1007/s10584-014-1080-9

Stott, P. (2016). How climate change affects extreme weather events. *Science* 352, 1517–1518. doi: 10.1126/science.aaf7271

Suh, K.-D., Kim, S.-W., Kim, S., and Cheon, S. (2013). Effects of climate change on stability of caisson breakwaters in different water depths. *Ocean Eng.* 71, 103–112. doi: 10.1016/j.oceaneng.2013.02.017

Takagi, H., Kashihara, H., Esteban, M., and Shibayama, T. (2011). Assessment of future stability of breakwaters under climate change. *Coast. Eng. J.* 53, 21–39. doi: 10.1142/S0578563411002264

Taylor, K. E., Stouffer, R. J., and Meehl, G. A. (2012). An overview of CMIP5 and the experiment design. *B. Am. Meteorol. Soc* 93, 485–498. doi: 10.1175/BAMS-D-11-00094.1

Thotagamuwage, D. T., and Pattiaratchi, C. B. (2014). Influence of offshore topography on infragravity period oscillations in Two Rocks Marina, Western Australia. *Coast. Eng.* 91, 220–230. doi: 10.1016/j.coastaleng.2014.05.011

Tolman, H. L. (2002). Alleviating the Garden Sprinkler effect in wind wave models. *Ocean Model.* 4, 269–289. doi: 10.1016/S1463-5003(02)00004-5

Tsimplis, M. N., and Shaw, A. G. P. (2010). Seasonal sea level extremes in the Mediterranean Sea and at the Atlantic European coasts. *Nat. Hazards Earth Syst. Sci.* 10, 1457–1475. doi: 10.5194/nhess-10-1457-2010

Verschuur, J., Koks, E. E., and Hall, J. W. (2020). Port disruptions due to natural disasters: Insights into port and logistics resilience. *Trans. Res. D-TR. E.* 85, 102393. doi: 10.1016/j.trd.2020.102393

Visbeck, M. (2018). Ocean science research is key for a sustainable future. *Nat. Commun.* 9, 690. doi: 10.1038/s41467-018-03158-3

Vitousek, S., Barnard, P. L., and Limber, P. (2017). Can beaches survive climate change? *J. Geophys. Res. Earth Surf.* 122, 1060–1067. doi: 10.1002/2017JF004308

Vousdoukas, M. I., Mentaschi, L., Voukouvalas, E., Verlaan, M., Jevrejeva, S., Jackson, L. P., et al. (2018). Global probabilistic projections of extreme sea levels show intensification of coastal flood hazard. *Nat. Commun.* 9, 2360. doi: 10.1038/s41467-018-04692-w

Vousdoukas, M. I., Ranasinghe, R., Mentaschi, L., Plomaritis, T. A., Athanasiou, P., Luijendijk, A., et al. (2020). Sandy coastlines under threat of erosion. *Nat. Clim. Change* 10, 260–263. doi: 10.1038/s41558-020-0697-0

Vousdoukas, M. I., Voukouvalas, E., Annunziato, A., Giardino, A., and Feyen, L. (2016). Projection of storm surge levels along Europe. *Clim. Dyn.* 47, 3171–3190. doi: 10.1007/s00382-016-3019-5

Vousdoukas, M. I., Wziatek, D., and Almeida, L. P. (2012). Coastal vulnerability assessment based on video wave run-up observations at a mesotidal, steep-sloped beach. *Ocean Dyn.* 62, 123–137. doi: 10.1007/s10236-011-0480-x

Wolff, C., Vafeidis, A. T., Muis, S., Lincke, D., Satta, A., Lionello, P., et al. (2018). Mediterranean coastal database for assessing the impacts of sea-level rise and associated hazards. *Sci. Data* 5, 180044. doi: 10.1038/sdata.2018.44

Woo, S.-B., and Liu, P. L.-F. (2004). Finite-element model for modified Boussinesq equations. II: applications to nonlinear harbor oscillations. *J. Waterw. Port Coast. Ocean Eng.* 130, 1–17. doi: 10.1061/(ASCE)0733-950X(2004)130:1(1

Yang, Z., Ng, A. K. Y., Lee, P. T.-W., Wang, T., Qu, Z., Sanchez Rodrigues, V., et al. (2018). Risk and cost evaluation of port adaptation measures to climate change impacts. *Transport Res. D-Tr. E.* 61, 444–458. doi: 10.1016/j.trd.2017.03.004

Yin, J., Griffies, S. M., and Stouffer, R. J. (2010). Spatial variability of sea level rise in twenty-first century projections. *J. Climate* 23, 4585–4607. doi: 10.1175/2010JCLI3533.1

Zheng, Z., Ma, X., Ma, Y., and Dong, G. (2020). Wave estimation within a port using a fully nonlinear Boussinesq wave model and artificial neural networks. *Ocean Eng.* 216, 108073. doi: 10.1016/j.oceaneng.2020.108073

Zviely, D., Bitan, M., and DiSegni, D. M. (2015). The effect of sea-level rise in the 21st century on marine structures along the Mediterranean coast of Israel: an evaluation of physical damage and adaptation cost. *Appl. Geogr.* 57, 154–162. doi: 10.1016/j.apgeog.2014.12.007